

## Contact Instability of the Direct Drive Robot When Constrained by a Rigid Environment

H. Kazerooni, S. Kim

111 Church Street SE  
Mechanical Engineering Department  
University of Minnesota  
Minneapolis, MN 55455

### ABSTRACT

Robot manipulations require mechanical interaction with the environment (i.e., the object being manipulated) which can constrain the robot endpoint in some or all directions. A sufficient condition for the stability of robot manipulators in constrained maneuvers is derived in the work presented here. Attention is focused on the class of direct drive robots whose rigid links dominate the robot's dynamic behavior; compared to the robot, the environment is assumed to be infinitely rigid. The stability of the manipulator-environment system is investigated, and a bound for stable manipulation is determined. This bound is verified experimentally on the Minnesota direct drive robot.

### 1. INTRODUCTION

Both fast motion in unconstrained space and mechanical interaction with the environment (i.e., the object being manipulated) are required in most robotic manufacturing tasks. Robotic assembly is an example of such a task where the robot must follow a trajectory when unconstrained by the environment, but, during the insertion process, the robot must comply with the environmental constraints. Robotic deburring (Kazerooni et al. 1986b) is another example of such a task where the interaction force<sup>1</sup> must be accommodated rather than resisted.

Whitney (1987) suggested two methods for implementing compliant motion. The first method controls force and position in a nonconflicting way (Mason 1981, Mills and Goldenberg 1989, Paul and Shimano 1976, Raibert and Craig 1981, Whitney 1977): force is commanded along those directions constrained by the environment, while position is commanded along those directions in which the manipulator is free to move. The second method develops a relationship between the interaction force and the manipulator position (Hogan 1985 and 1987, Kazerooni 1986a, 1989b, Kazerooni and Tsay 1988, Salisbury 1980): by controlling the manipulator position and specifying its relationship with the interaction force, a designer ensures that the manipulator can maneuver in a constrained space while maintaining appropriate contact force. This paper analyzes the stability of the robot-environment system when the second method is employed to control robot compliancy. A sufficient condition for system stability is derived analytically and verified experimentally on a direct drive robot arm. References 5, 11, 12, and 13 give some preliminary results on the stability of robotic constrained maneuvers. An and Hollerbach (1987) and Colgate (1988) discuss stability analysis for linear, single-degree-of-freedom systems.

<sup>1</sup>In this article, "force" implies force and torque, and "position" implies position and orientation.

### 2. UNCONSTRAINED ANALYSIS

The dynamic behavior of direct drive robots with  $n$  degrees of freedom is expressed by equation 1:

$$M(\theta) \ddot{\theta} + C(\theta, \dot{\theta}) = \tau - J^T f \quad (1)$$

where  $\ddot{\theta}$ ,  $\dot{\theta}$ ,  $\theta$  are vectors containing the joints' accelerations, velocities, and positions;  $M(\theta)$  is the inertia matrix;  $C(\theta, \dot{\theta})$  is the vector representing the coriolis, centrifugal, and gravity forces;  $\tau$  is the vector of joint torques;  $J^T$  is the Jacobian transpose matrix; and  $f$  is the vector of external forces applied at the robot endpoint (Hollerbach 1980). Trajectory control of the manipulator is performed by a digital implementation of a feedforward torque controller, which torque is given by:

$$\tau = K_p (\theta_d - \theta) + K_v (\dot{\theta}_d - \dot{\theta}) + \dot{M}(\theta_d) \ddot{\theta}_d + \dot{C}(\theta_d, \dot{\theta}_d) \quad (2)$$

where  $\tau$  is the vector of joint torques;  $(\theta_d - \theta)$  is the error between the command position,  $\theta_d$ , and the actual position,  $\theta$ , and  $(\dot{\theta}_d - \dot{\theta})$  is the error between the respective velocities;  $K_p$  is an  $n \times n$  matrix containing the position gains;  $K_v$  is an  $n \times n$  matrix containing the velocity gains;  $\dot{M}(\theta_d)$  and  $\dot{C}(\theta_d, \dot{\theta}_d)$ , which can be found experimentally or analytically, are educated guesses for  $M(\theta)$  and  $C(\theta, \dot{\theta})$ . The nonlinear feedforward terms,  $\dot{M}(\theta_d)$  and  $\dot{C}(\theta_d, \dot{\theta}_d)$ , cancel the nonlinear effects of  $M(\theta)$  and  $C(\theta, \dot{\theta})$  in the robot's dynamics and result in a nearly uncoupled linear system (Spong and Vidyasagar, 1985). In feedforward torque control, the robot trajectory is specified in joint coordinates, and the joint positions, velocities, and accelerations for a given trajectory are computed and stored before the trajectory is executed. The  $\text{Kin}(\cdot)$  operator in the diagram represents the forward kinematics, while  $\text{Kin}^{-1}(\cdot)$  represents the inverse kinematics. When the trajectory is specified in Cartesian space as a function of time,  $e(t)$ , inverse kinematics and numerical differentiation transform it into the joint space,  $\theta_d(t)$ .

$$\theta_d(t) = \text{kin}^{-1} [ e(t) ] \quad (3)$$

$$\dot{\theta}(t) = \text{kin} [ \dot{\theta}(t) ] \quad (4)$$

The nonlinear control law of equation 2 is chosen because the inertia and coriolis terms can be computed and stored. During the trajectory execution, these terms are added to the error terms to compute the joint torques. The chief advantage of this approach is

that only a modest amount of computation must be performed in real time and the sampling time is correspondingly reduced.

Although computationally efficient, feedforward torque control does not achieve perfect uncoupling of each joint. Using equations 1 and 2 and assuming that  $\hat{C}(\theta_d, \dot{\theta}_d) \approx C(\theta, \dot{\theta})$  and  $\hat{M}(\theta_d) \approx M(\theta)$ , a differential equation in terms of the joint accelerations is obtained:

$$J^T f = K_p (\theta_d - \theta) + K_v (\dot{\theta}_d - \dot{\theta}) + M(\theta) (\ddot{\theta}_d - \ddot{\theta}) \quad (5)$$

where  $M(\theta)$  is a symmetric, positive definite matrix whose inverse exists for all robot configurations,  $\theta$ . Despite the assumption that the robot dynamics are accurately known, the joints are not perfectly uncoupled, and the degree of coupling varies as a function of the robot configuration. If  $K_p$  and  $K_v$  are chosen as positive definite matrices, the robot dynamic behavior will be  $L_2$  stable, and  $(\theta_d - \theta)$  will be an  $L_2$  bounded quantity even in the presence of nonzero, but bounded, uncertainties in computing  $\hat{C}(\theta_d, \dot{\theta}_d)$  and  $\hat{M}(\theta_d)$ .

### 3. CONSTRAINED ANALYSIS

Figure 1 shows the robot interacting with the environment where the robot compliancy is created by an H compensator. The environment produces a force,  $f$ , which is expressed in the global Cartesian coordinate frame as  $f = E(x)$ . In many applications,  $f$  may be zero if  $x$  is negative. For example, in the grinding of a surface, if positive  $f_1$  is "pushing" and negative  $f_1$  is "pulling", the robot and the environment contact each other only along those directions where  $f_i > 0$  for  $i=1, \dots, n$ . In some applications, such as turning a bolt, the interaction force can be either positive or negative, meaning that the interaction torque can be either clockwise or counterclockwise. The nonlinear discriminator block diagram in Figure 1 is drawn with a dashed line to represent the above concept; the block is present only when the interaction forces are compressive. Reference 10 represents  $(Is^2 + Ds + K)$  for the environment dynamics,  $E$ , where  $I$ ,  $D$  and  $K$  are symmetric matrices and  $s = j\omega$  (Lancaster 1966).  $I$  is the positive definite inertia matrix, and  $D$  and  $K$  are the positive semi-definite damping matrix and the stiffness matrix.

Although the trajectory controller operates in the manipulator joint space,  $H$  is implemented as a transfer function matrix.  $H$  accepts the Cartesian force and produces a signal representing a Cartesian displacement which subtracts from the commanded trajectory such that  $e(t) = r(t) - Hf(t)$ . The input command vector,  $r$ , is used differently for the two types of maneuvers: as a command to specify the input trajectory in unconstrained maneuvers and as a command to control force in constrained maneuvers. This method is referred to as Impedance Control because it accepts a position vector as input and it returns a force vector as output. There is no hardware or software switch in the control system when the robot travels between unconstrained space and constrained space. When the robot encounters the environment, the feedback loop on the contact force closes naturally. The contact force is shaped by the robot dynamics and the designers' choice of  $H$ . Depending on the task,  $H$  can take on various values in different directions. A small  $H$  generates a stiff robot and a large  $H$  results in a compliant robot (Kazerooni 1988). However,  $H$  cannot be arbitrarily large; the stability of the closed-loop system of Figure 1 must be guaranteed.

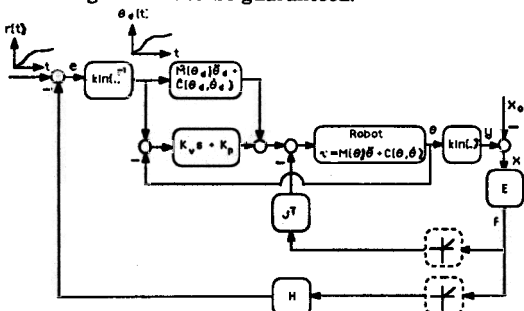


Figure 1: In constrained maneuvers, the contact force,  $f$ , affects the robot via two feedback loops.

When the robot contacts an infinitely stiff and stationary environment, the environment dictates the robot's position: in the constrained directions, the environment deflection,  $x$ , is zero and the robot position is the same as the environment position. In this analysis, the robot endpoint is assumed to be constrained by the environment in all directions; this represents the "worst" robot maneuver. Instability in this worst case is characterized by the unbounded oscillations of the contact forces while  $\theta$  remains a bounded quantity. The above are reflected in the following two equations:

$$\text{kin}[\theta(t)] = x_0 \quad (6)$$

$$\dot{\theta}(t) = \dot{\theta}(t) = 0 \quad (7)$$

Substituting  $\theta_d$ ,  $\theta$ ,  $\dot{\theta}(t)$ , and  $\ddot{\theta}(t)$  from equations 3, 6, and 7 into equation 5 and replacing  $e$  with  $(r - H^*(f))$  results in equation 8 where  $H^*(f)$  implies the convolution of the impulse response of  $H$  and  $f$ .

$$f = J^{-T} K_p \text{kin}^{-1} [r - H^*(f)] - J^{-T} K_p \text{kin}^{-1} [x_0] + J^{-T} K_v (\dot{\theta}_d) + J^{-T} M(\theta) \ddot{\theta}_d \quad (8)$$

When the robot is not in contact with the environment (i.e., the outer feedback loops in Figure 1 do not exist), the position of the robot endpoint is governed by equation 5. When the robot is in contact with the environment, the contact force follows  $r$  according to equation 8. If the trajectory command,  $r$ , extends a small distance beyond the solid environment,  $\text{kin}^{-1}$  can be replaced by  $J^{-1}$  and equation 8 can be written as:

$$f = J^{-T} K_p J^{-1} [r - H^*(f) - x_0] + J^{-T} K_v (\dot{\theta}_d) + J^{-T} M(\theta) \ddot{\theta}_d \quad (9)$$

Since the environment is infinitely stiff,  $E$  cannot be assumed to be an  $L_2$  stable operator. This prevents substituting for  $f$  (via the operator  $E$  as a function of  $x$  or  $\theta$ ) in equation 9. Instead,  $f$  is treated as the test parameter for the closed loop stability; if  $f$  is bounded in the  $L_2$  sense, then the system will be stable. In the case of finite  $E$ , one can substitute for  $f$ , and an equation similar to equation 5 can be obtained for stability analysis. The truncated  $L_2$  norm<sup>2</sup> of equation 9 is written as:

$$\|f\|_{T_2} \leq \sigma_{\max}(J^{-T} K_p J^{-1}) \|H^*(f)\|_{T_2} + \|J^{-T} K_p J^{-1} (r - x_0)\|_{T_2} + \|J^{-T} K_v (\dot{\theta}_d) + J^{-T} M(\theta) \ddot{\theta}_d\|_{T_2} \quad (10)$$

Since  $\theta$  is dictated by the environment,  $M(\theta)$  in equation 9 is a function of  $x_0$  and consequently will be bounded. Since  $r$ ,  $x_0$ ,  $\theta_d$ , and  $M(\theta)$  are bounded quantities, then the last two norms of inequality 10 will be bounded by a positive scalar,  $\beta$ , and inequality 10 can be written as:

$$\|f\|_{T_2} \leq \sigma_{\max}(J^{-T} K_p J^{-1}) \|H^*(f)\|_{T_2} + \beta \quad (11)$$

<sup>2</sup> The  $L_2$ -norm of an  $n \times 1$  vector function  $f(t)$  is defined as [Vidyasagar 1978, Vidyasagar and Desoer, 1975]:

$$\|f\|_2 = \left[ \int_0^{\infty} |f(t)|^2 dt \right]^{1/2}$$

Where  $|f(t)|$  is the Euclidean norm evaluated at a given time  $t$ . If  $\|f\|_2 \leq \infty$ , then  $f \in L_2^n$ . For functions that may grow unboundedly, a truncated  $L_2$ -norm is defined:

$$\|f\|_{T_2} \triangleq \|f(t)\|_2, \quad 0 \leq t < T$$

$\|H^*(f)\|_{r2}$  can be replaced with  $\sigma_{\max}(Q) \|f\|_{r2}$  where  $\sigma_{\max}(Q)$  is the maximum singular value<sup>3</sup> of  $Q$  and  $Q$  is a matrix whose entry  $(i,j)$  is given by  $(Q)_{ij} = \sup_{\omega} |H(j\omega)_{ij}|$ . The closed loop system of Figure 1 is  $L_2$  stable ( $f$  is  $L_2$  bounded) if inequality 12 is satisfied over the commanded trajectory.

$$\sigma_{\max}(J^{-T} K_p J^{-1}) \sigma_{\max}(Q) < 1 \quad (12)$$

$$\sigma_{\max}(Q) < \frac{1}{\sigma_{\max}(J^{-T} K_p J^{-1})} \text{ (over the commanded trajectory)} \quad (13)$$

Equivalently, one can satisfy inequality 14.

$$\sigma_{\max}(Q) < \text{infimum of } \sigma_{\min}(J K_p^{-1} J^T) \text{ (over the commanded trajectory)} \quad (14)$$

The minimum singular value of  $(J K_p^{-1} J^T)$  must be calculated at each point in the commanded trajectory. The infimum is the lowest of all the minimum singular values. The gain of  $H$ , expressed in terms of  $\sigma_{\max}(Q)$ , must be chosen to be smaller than this infimum. From inequality 14, the stability region will approach zero when the robot maneuvers near a singular point ( $\det(J) \rightarrow 0$ ) and/or when the position gains approach infinity. Both cases are representative of "infinite stiffness" for the robot; the first is due to the robot configuration, while the second is due to the tracking controller. The above stability condition has been extended to robots with unstructured models (Kazerooni and Tsay 1988).

#### 4. EXPERIMENTAL RESULTS

To evaluate the nonlinear stability condition, a compliance controller is implemented on a direct-drive, three-degree-of-freedom robot (Kazerooni and Kim 1988 and 1989a). The University of Minnesota direct drive robot (Figure 2) uses a four-bar linkage and is statically balanced without any counter weights. As a result of the elimination of the gravity forces, smaller actuators and, thus, smaller amplifiers were chosen to drive this robot. The motors yield acceleration of 5g at the endpoint without overheating. High torque, low speed motors power the robot; specifically, the motors are neodymium (NdFeB) magnet AC brushless synchronous motors. Due to the high magnetic field strength (maximum energy products: 35 MGOe) of the rare earth NdFeB magnets, the motors have high torque-to-weight ratios. Pancake-type resolvers are used as position and velocity sensors. The peak torque of motors 1, 2, and 3 are 118 Nm, 78 Nm, and 58 Nm, respectively. The robot links are made of graphite-epoxy composite material. A microcomputer, which hosts a 4-node parallel processor with a PC/AT bus interface, is the main robot controller. Each node is an independent 32-bit processor with local memory and communication links to the other nodes in the system.

Because this robot has no gears, frictional losses are small and the manipulator can be modeled by equation 1. For a sufficient stability condition, if the condition is satisfied, stability is guaranteed; however, if the condition is violated, no conclusion can be made. Two experiments are performed to demonstrate that inequality 14 is a sufficient condition for stability: one experiment in which the satisfaction of the condition leads to a stable maneuver and one experiment in which parameters for an unstable maneuver violate the condition. In the first experiment, an  $H$  is designed such that inequality 14 is satisfied and it is shown, through experiment, that the system is stable. In the second experiment, it is shown that an  $H$  which destabilizes the system also violates inequality 14.

A reinforced aluminum wall is mounted vertically in the robot workspace, as shown in Figure 2, to simulate a stiff environment. Motor 2 is mechanically locked while motors 1 and 3 maneuver the robot endpoint horizontally. A piezoelectric force sensor is mounted on the manipulator endpoint to measure contact forces.

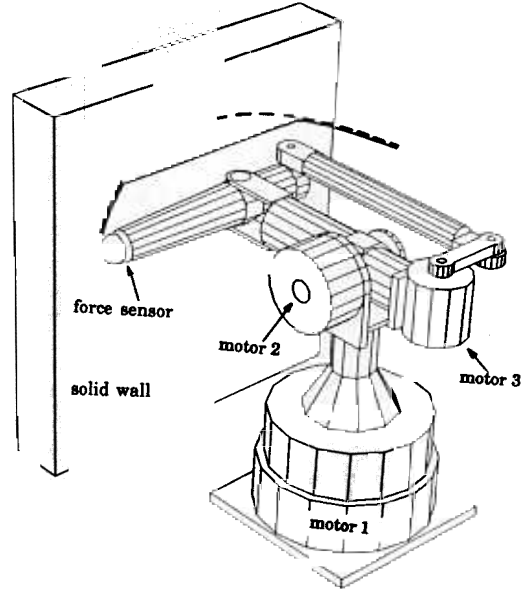


Figure 2: The dashed line is the desired endpoint trajectory while the solid line is the actual trajectory.

Since the experiments are all two-dimensional,  $H$  is a  $2 \times 2$  matrix operating on contact forces which are normal and tangential to the wall. (The endpoint force measurements are resolved into the global coordinate frame.) In these experiments, only the compliancy in the direction normal to the wall is supplemented, so the following form of  $H$  is chosen:

$$H = \begin{bmatrix} \frac{H_0}{Ts+1} & 0 \\ 0 & 0 \end{bmatrix} \quad (15)$$

where  $T$  is an empirical constant and filters high frequency noise in the force measurement.  $T$  is fixed at 0.05 for all the experiments. The function  $r(t)$ , shown in Figure 2 by the dashed line, is the trajectory assigned to the robot. Since  $H$  has only one non-zero member, then  $\sigma_{\max}(Q)$  will be the maximum value of the magnitude of  $H_0/(Tj\omega + 1)$ . The maximum value of  $H$  is  $H_0$  and occurs at DC ( $\omega=0$ ).

In the first experiment, it is shown that if inequality 14 is satisfied for the maneuver shown in Figure 2, then the robot can have stable interaction with the environment.  $H_0$  is chosen to be .0003 so  $H(s)$  is smaller than  $\sigma_{\min}(J K_p^{-1} J^T)$  for all configurations within the maneuver. Figure 3 shows the experimental values of the normal contact force. Stable contact is indicated by the absence of undamped oscillations in the normal force.

In the second experiment,  $H_0$  is set to .0015. Figure 4 shows the experimental normal contact force as a function of time. The contact force oscillates throughout the maneuver, indicating that the compliance controller is unstable. Comparison with the singular value plots of  $J K_p^{-1} J^T$  shows that  $H_0$  exceeds the lower bound on  $\sigma_{\min}(J K_p^{-1} J^T)$ ; hence, the stability condition is violated. Since inequality 14 is a sufficient condition for stability, violation of this condition does not lead to any conclusion. The system can be stable even if the stability condition is not satisfied as in Figure 5, which shows the experimental contact forces when  $H_0=0.0005$ .

<sup>3</sup> The maximum singular value of a matrix  $H$ ,  $\sigma_{\max}(H)$  is defined as:

$$\sigma_{\max}(H) = \max \frac{|Hz|}{|z|}, \quad z \neq 0$$

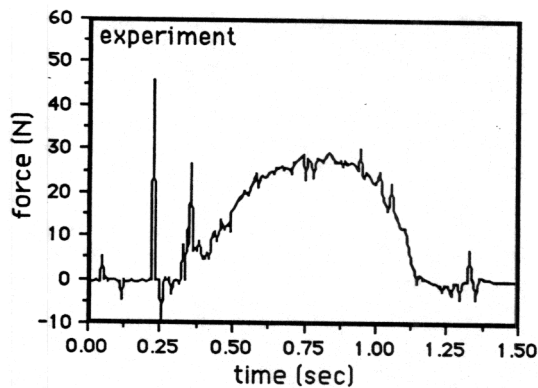


Figure 3:  $H_0 = 0.0003$  satisfies the stability condition.

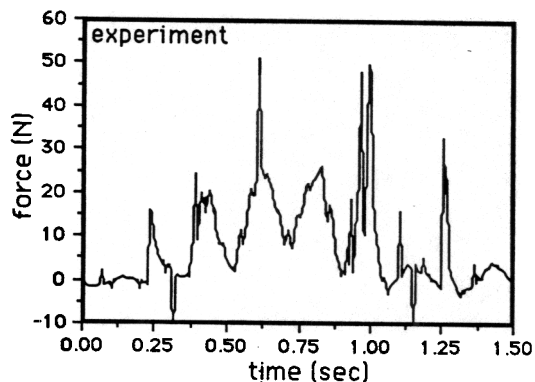


Figure 4:  $H_0 = 0.0015$  does not satisfy the stability condition.

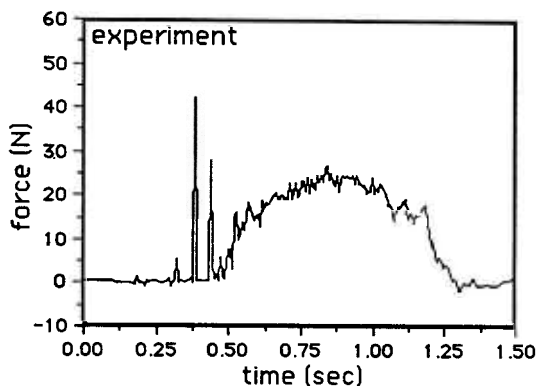


Figure 5:  $H_0 = 0.0005$  violates the stability condition; however, the system is stable.

## 5. SUMMARY AND CONCLUSION

An architecture for compliance control of direct drive robot manipulators is presented. The control approach allows not only tracking the input command vector in unconstrained space, but also compliancy in constrained maneuvers. A bound for the global stability of the robot and infinitely stiff environment, taken together, is derived. The stability region theoretically will approach zero when the robot maneuvers near its singular point and/or the position gain approaches infinity. Both cases are representative of infinite stiffness for the robot. Through both simulation and experimentation, the sufficiency of this condition is demonstrated.

## REFERENCES

1) An, C. H., Hollerbach, J. M., "Dynamic Stability Issues in Force Control of Manipulators", IEEE International Conference

on Robotics and Automation, pp. 890-896, Raleigh, NC, March 1987.

- 2) Colgate, J. E., Hogan, N., "Robust Control of Dynamically Interacting Systems", International Journal of Control, Volume 48, Number 1, July 1988.
- 3) Hollerbach, J. M., "A Recursive Lagrangian Formulation of Manipulator Dynamics and a Comparative Study of Dynamics Formulation Complexity", IEEE Trans. on Systems, Man and Cybernetics Volume 10, Number 11, pp. 730-736, November, 1980.
- 4) Hogan, N., "Impedance Control: An Approach to Manipulation", ASME Journal of Dynamic Systems, Measurement, and Control, Volume 107, Number 1, pp. 1-24, March 1985.
- 5) Hogan, N., "On the Stability of Manipulators Performing Contact Tasks", Conference on Applied Motion Control, Minneapolis, MN, June 1987.
- 6) Kazerooni, H., "Fundamentals of Robust Compliant Motion for Manipulators", IEEE Journal of Robotics and Automation, Volume 2, Number 2, June 1986a.
- 7) Kazerooni, H., Bausch, J. J., Kramer, B. K., "An Approach to Automated Deburring by Robot Manipulators", ASME Journal of Dynamic Systems, Measurements and Control, Volume 108, Number 4, December 1986b.
- 8) Kazerooni, H., Tsay, T. I., "On the Stability of the Constrained Robotic Maneuver", American Control Conference, Atlanta, Georgia, pp 892-897, June 1988.
- 9) Kazerooni, H., "Direct Drive Active Compliant End-Effector", IEEE Journal of Robotics and Automation, Volume 4, Number 3, June 1988.
- 10) Kazerooni, H. and Kim, S., "A New Architecture for Direct Drive Robots", IEEE International Conference on Robotics and Automation, Volume 1, pp.442-445, Philadelphia, PA, April 1988.
- 11) Kazerooni, H., "Design and Analysis of the Statically Balanced Direct Drive Manipulator," IEEE Control System Magazine, Volume 9, Number 2, February 1989a.
- 12) Kazerooni, H. "On the Robot Compliant Motion Control," ASME Journal of Dynamic Systems, Measurements, and Control, Volume 111, Number 3, September 1989b.
- 13) Lancaster, P., Lambda-Matrices and Vibrating Systems. Pergamon Press, 1966.
- 14) Mason, M. T., "Compliance and Force Control for Computer Controlled Manipulators", IEEE Transaction on Systems, Man, and Cybernetics SMC-11(6):418-432, June, 1981.
- 15) Mills, J. K., Goldenberg, A. A., "Force and Position Control of Manipulators During Constrained Motion Tasks", IEEE Transaction on Robotics and Automation, Volume 5, Number 1, February 1989.
- 16) Paul, R. P. C., Shimano, B., "Compliance and Control", In Proceedings of the Joint Automatic Control Conference, pages 694-699. San Francisco, 1976.
- 17) Raibert, M. H., Craig, J. J., "Hybrid Position/Force Control of Manipulators", ASME Journal of Dynamic Systems, Measurement, and Control Volume 102, June 1981.
- 18) Salisbury, K. J., "Active Stiffness Control of Manipulator in Cartesian Coordinates", In Proceedings of the 19th IEEE Conference on Decision and Control, pages 95-100, Albuquerque, New Mexico, December 1980.
- 19) Spong, M. W., Vidyasagar, M., "Robust Nonlinear Control of Robot Manipulators", IEEE Conference on Decision and Control, December 1985.
- 20) Vidyasagar, M., "Nonlinear Systems Analysis", Prentice-Hall, 1978.
- 21) Vidyasagar, M., Desoer, C. A., "Feedback Systems: Input-Output Properties", Academic Press, 1975.
- 22) Whitney, D. E., "Force-Feedback Control of Manipulator Fine Motions", ASME Journal of Dynamic Systems, Measurement, and Control, pp. 91-97, June, 1977.
- 23) Whitney, D. E., "Historical Perspective and State of the Art in Robot Force Control," The International Journal of Robotics Research, Volume 6, Number 1, Spring 1987.